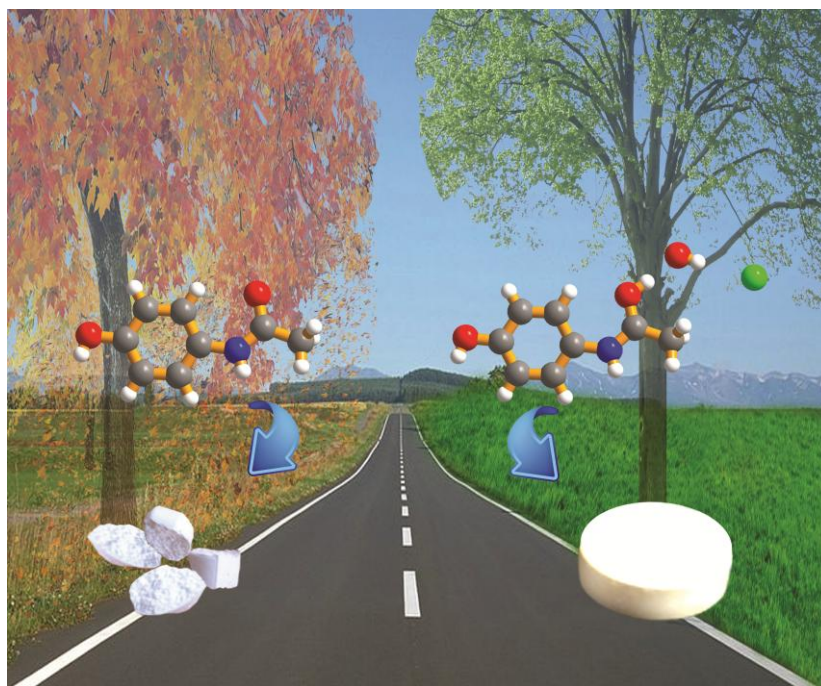


This article is published as part of the *CrystEngComm* themed issue entitled:

## Crystal Engineering and Crystallography in the Pharmaceutical Industry

Guest Editors Magali Hickey, Örn Almarsson and Matt Peterson

Published in [issue 7, 2012](#) of *CrystEngComm*



Articles in this issue include:

### Highlight

[The role of mechanochemistry and supramolecular design in the development of pharmaceutical materials](#)

Amit Delori, Tomislav Friščić and William Jones

### Highlight

[Pharmaceutical crystallography: is there a devil in the details?](#)

Andrew D. Bond

### Paper

[The effect of water molecules in stabilizing co-crystals of active pharmaceutical ingredients](#)

Christer B. Aakeröy, Safiyyah Forbes and John Desper

Visit the *CrystEngComm* website for more cutting-edge crystal engineering research

[www.rsc.org/crystengcomm](http://www.rsc.org/crystengcomm)

Cite this: *CrystEngComm*, 2012, **14**, 2428

www.rsc.org/crystengcomm

PAPER

# Sodium and potassium salts of bumetanide trihydrate: Impact of counterion on structure, aqueous solubility and dehydration kinetics†

Winston Ong,<sup>‡\*</sup> Eugene Y. Cheung, Karen A. Schultz, Cartney Smith, James Bourassa and Magali B. Hickey

Received 6th December 2011, Accepted 10th February 2012

DOI: 10.1039/c2ce06631a

A form of bumetanide potassium trihydrate that is structurally similar to bumetanide sodium trihydrate was identified. Structural analysis indicated however that the change from sodium to potassium salt resulted in meaningful changes in the packing arrangement and even greater changes on physicochemical properties. The potassium trihydrate salt was five times more soluble in water relative to the sodium trihydrate salt (27 mg mL<sup>-1</sup> vs. 5.6 mg mL<sup>-1</sup>). Both salts underwent complete dehydration to their corresponding anhydrate forms following exposure to low humidity or elevated temperature. Arrhenius plots for the dehydration between 20–30 °C yielded a lower activation barrier for the potassium trihydrate compared to the sodium trihydrate (14.9 kcal mol<sup>-1</sup> vs. 19.9 kcal mol<sup>-1</sup>), translating into a 15–20-fold difference in the rate of dehydration. Such a 5.0 kcal mol<sup>-1</sup> gap suggests that the H<sub>2</sub>O molecules are more tightly bound in the sodium trihydrate compared to potassium trihydrate. These differences in solubility and rate of dehydration further illustrate that changes to chemical composition can have a meaningful and unpredictable impact on the physicochemical properties of closely related pharmaceutical salt forms.

## Introduction

Utilization of salts is a common strategy to enhance the solubility of low-molecular weight (MW) active pharmaceutical ingredients (APIs).<sup>1–4</sup> In their neutral forms, ionizable APIs may suffer from sub-optimal pharmaceutical properties, such as slow dissolution rate and low solubility in aqueous systems, often resulting in poor oral bioavailability.<sup>5–9</sup> In addition, drug products that require reconstitution at the point of administration often depend on the identification of a high-solubility salt. For this reason, APIs intended for parenteral administration require extensive salt screening to ensure that a suitable form is selected for development.

Bumetanide<sup>10</sup> (Fig. 1) is a potent loop diuretic with rapid onset and short duration of action. It is indicated to manage oedema typically associated with congestive heart failure, hepatic and renal disease, and to treat mild to moderate hypertension.<sup>11</sup>

*Transform Pharmaceuticals, Inc. (A Johnson & Johnson company), 29 Hartwell Avenue, Lexington, MA 02421, USA*

† Electronic supplementary information (ESI) available: Thermogravimetric and differential scanning calorimetric thermograms of bumetanide K and bumetanide Na(H<sub>2</sub>O)<sub>3</sub>, conversion between trihydrate and anhydrate states of the sodium and potassium salts under various humidities and temperatures, and raw solubility data of bumetanide, bumetanide K(H<sub>2</sub>O)<sub>3</sub> and bumetanide Na(H<sub>2</sub>O)<sub>3</sub>. CCDC reference number 857276. For ESI and crystallographic data in CIF or other electronic format see DOI: 10.1039/c2ce06631a

‡ Present address: Kala Pharmaceuticals, Inc., 135 Beaver St, Suite 309, Waltham, MA, 02452 USA; Fax: +781-642-0399; Tel: +781-996-5255; E-mail: winston.ong@kalarx.com

Currently prescribed as the free acid in solid oral dosage and injectable forms, bumetanide has low aqueous solubility (0.1 mg mL<sup>-1</sup>),<sup>12</sup> which subsequently limits its utility in low-volume injectable delivery. Though bumetanide sodium trihydrate<sup>13</sup> was independently determined to have an aqueous solubility of 5.6 mg mL<sup>-1</sup>, which is significantly more soluble than the free acid, identification of alternative salts with higher aqueous solubilities could facilitate the development of low-volume, parenteral formulations of bumetanide.

It has been shown recently that a change in counter-ion of low-MW APIs can lead to a significant change in crystal packing.<sup>14</sup> In fact, the swapping of a sodium cation for potassium during salt formation was found to, more often than not, result in significant differences in packing arrangements. While such analysis illustrates that subtle variations in chemical composition can be expected to change the packing arrangement, the magnitude of the change and the impact on the physicochemical properties of the resultant materials remains highly unpredictable.<sup>15</sup>

Herein, the crystal structure and physicochemical properties of bumetanide potassium trihydrate (bumetanide K(H<sub>2</sub>O)<sub>3</sub>) are reported. Though the structure was found to be similar in terms

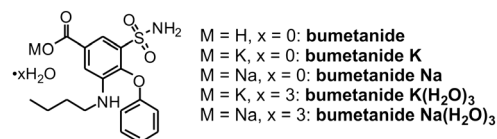


Fig. 1 Structure of bumetanide and bumetanide salts.

of space group and overall packing arrangement to the corresponding sodium salt trihydrate (**bumetanide Na(H<sub>2</sub>O)<sub>3</sub>**),<sup>13</sup> the structures were neither identical nor isostructural. The physico-chemical properties of the sodium and potassium trihydrate salts drastically differ as follows: (i) the potassium salt is five times more soluble in water at pH > 7.5 (ii) the potassium salt dehydrates 15–20 times faster, and (iii) the sodium salt is the only trihydrate that is physically stable under ambient conditions (22 °C and 30–50% RH). Crystal structure analysis was conducted to provide insight into the aforementioned difference in solubility, dehydration rate and physical stability.

## Methods and materials

Bumetanide was obtained from AK Scientific (Union City, CA). Sodium hydroxide and potassium hydroxide were purchased from Aldrich (St. Louis, MO) as 1.0 M solutions. Solvents were HPLC grade and were purchased from EMD Chemicals (Gibbstown, NJ).

### Preparation of the bumetanide salts

**Potassium salt anhydrate (bumetanide K).** Aqueous potassium hydroxide (13.3 mL × 1.0 M) was added drop wise to a stirred solution containing bumetanide (4.89 g, 13.3 mmol) dissolved in methanol (150 mL) at ambient temperature. After stirring the solution for 5 min, the solvent was evaporated under reduced pressure to produce the anhydrous salt as a white solid. Isolated yield: 5.37 g (11.8 mmol, 89%).

**Sodium salt trihydrate (bumetanide Na(H<sub>2</sub>O)<sub>3</sub>).** This salt was prepared in the same manner as **bumetanide K**, except that sodium hydroxide (13.3 mL × 1.0 M) was used in place of potassium hydroxide. Isolated yield starting from bumetanide free acid (4.91 g, 13.3 mmol) was 5.80 g (13.2 mmol, 99%). The crystal structure of this salt has previously been deposited in the Cambridge Structural Database as WINJAE.<sup>13</sup>

**Potassium salt trihydrate (bumetanide K(H<sub>2</sub>O)<sub>3</sub>) single crystals.** **Bumetanide K** was dissolved in H<sub>2</sub>O at 50 °C to generate a 50-mg mL<sup>-1</sup> solution, which was then allowed to spontaneously equilibrate to ambient temperature. Needle-shaped crystals of **bumetanide K(H<sub>2</sub>O)<sub>3</sub>** started growing after 24 h.

**Sodium salt anhydrate (bumetanide Na).** Exposure of 15–25 mg of **bumetanide Na(H<sub>2</sub>O)<sub>3</sub>** to 0% relative humidity (RH, at 25 °C) or >80 °C in the variable humidity or variable temperature chambers of a Bruker D8 Advance diffractometer (see below) generated the anhydrate salt *in situ*, as observed by the emergence of new PXRD peaks.

### Powder X-ray diffraction (PXRD)

High-resolution PXRD patterns were obtained using the D/Max Rapid X-ray Diffractometer equipped with a copper source (Cu/K $\alpha$  1.5418 Å), manual x–y stage, and 0.3-mm collimator. Samples were loaded into a 0.3-mm boron rich glass capillary tube by sectioning off one end of the tube and tapping the open, sectioned end into a bed of sample. The loaded capillary was mounted in a holder secured into the x-y stage. Diffractograms

were acquired under ambient conditions (22 °C and 30–50% RH) at a power setting of 46 kV at 40 mA in reflection mode, while oscillating about the omega-axis from 0–5° at 1°/s and spinning about the phi-axis at 2°/s. Exposure time was 5 min. The diffractograms were integrated over 2-theta from 2–40° and chi (1 segment) from 0–360° at a step size of 0.02° using the *cylint* utility in the RINT Rapid display software provided with the instrument. The dark counts value was set to 8 as per the system calibration; normalization was set to average; the omega offset was set to 180°; and no chi or phi offsets were used for the integration. Variable temperature and variable humidity PXRD data were obtained on a Bruker D8 Advance X-ray diffractometer with Sol-X detector equipped with a Parr TTK-450 and MRI-700900 chamber, respectively. Samples were scanned from 3.5–40° (0.02°/step and 0.65 s/step) at 45 kV and 40 mA with Cu-K $\alpha$  radiation (1.54 Å).

### Single crystal X-ray diffraction

The specimen chosen for X-ray diffraction study was a clear, colorless needle measuring 0.049 × 0.077 × 0.573 mm. Single crystal data were collected at 100 K on a Bruker kappa APEX II diffractometer system supplied with a Mo-K $\alpha$  fine-focus sealed X-ray tube ( $\lambda$  = 0.71069 Å) and operated at 50 kV, 30 mA. Frames were collected with a scan width of 0.5° in  $\omega$  and an exposure time of 20 s/frame. A total of 2180 frames were integrated. The total data collection was 24 h. The crystal structure was solved by direct methods and refined by least squares using CRYSTALS.<sup>16</sup> Hydrogen atoms were located by Fourier difference or calculated in idealized positions. The refinement converged at  $R$  = 0.0360,  $R_w$  = 0.0697, for 7515 independent reflections with  $I \geq 2\sigma$  and 262 variables.

### Dynamic Vapor Sorption (DVS)

Vapor sorption–desorption data of approximately 10 mg of bumetanide salt were acquired using DVS-1 (Surface Measurement Systems, Allentown, PA). The instrument was allowed to equilibrate for at least an hour at each temperature prior to the start of the experiment. Humidity steps were ramped in 10% increments after the change in mass ( $dM/dT$ ) fell under 0.02% within a ten-minute window. The activation energy ( $E_a$ ) for the removal of H<sub>2</sub>O from the crystal lattices of **bumetanide Na(H<sub>2</sub>O)<sub>3</sub>** and **bumetanide K(H<sub>2</sub>O)<sub>3</sub>** was determined using the classical Arrhenius method,<sup>17</sup> which consisted of isothermal dehydration experiments performed over a series of temperatures (approximately 30 °C, 27.5 °C, 25 °C and 20 °C). The initial humidity setting for the Na salt corresponded to an absolute vapor pressure equivalent to 30%  $P/P^0$  at 25 °C, where  $P$  is the actual vapor pressure and  $P^0$  is the saturated vapor pressure. The initial humidity setting for the K salt was 90%  $P/P^0$  at all temperatures. Dehydration was initiated by switching the initial humidity setting to 100% N<sub>2</sub> (*i.e.*, 0%  $P/P^0$ ). Zero-order rates of dehydration ( $k$ ) were extracted from data points covering 0–75% dehydration using the least squares method. Each dehydration measurement was obtained in triplicate. Least squares analysis of the corresponding Arrhenius plots ( $\ln(k)$  vs.  $T^{-1}$ ) generated slopes equal to  $-E_a/R$ , where  $R$  is the universal gas constant.

## Solubility

The pH-solubility profiles starting from **bumetanide K** and **bumetanide Na(H<sub>2</sub>O)<sub>3</sub>** were determined from buffer-free suspensions stirred at ambient temperature (22 °C) for 24 h. Drug substance was suspended in de-ionized water (1 mL) in a 3-mL vial equipped with a magnetic stir bar and pH was adjusted by titrating the suspensions with 0.1 M HCl or the appropriate hydroxide base (0.1 M KOH or 0.1 M NaOH). After stirring the suspension for 24 h, the pH was measured, undissolved solids were separated from the mixture *via* filtration using a 0.2- $\mu$ m PTFE membrane, and the solution was diluted 2–1000-fold for LC (liquid chromatography) analysis. The starting concentrations of the suspensions varied according to the target pH as follows: at pH < 5, the initial concentrations were 6 mg mL<sup>-1</sup> for both Na and K salts, while at pH > 5, the initial concentrations were 20 mg mL<sup>-1</sup> and 50 mg mL<sup>-1</sup> for the Na and K salts, respectively.

## Liquid chromatography

Bumetanide content was determined using a Waters ACQUITY Ultra Performance LC system equipped with a PDA detector. A 2.1 mm  $\times$  50 mm BEH C18 column with particle size of 1.7  $\mu$ m was used and maintained at 40 °C. Mobile phase A consisted of 0.1% formic acid in H<sub>2</sub>O, while mobile phase B was 0.1% formic acid in CH<sub>3</sub>CN. The flow program consisted of a two-minute gradient of 60% to 10% mobile phase A at 0.7 mL min<sup>-1</sup>. Analysis was performed with a 5- $\mu$ L injection, and quantitation was based on an extracted wavelength of 268 nm.

## Results and discussion

### Characterization and physical stability of bumetanide salts

The PXRD patterns of bumetanide and its various salt forms are shown in Fig. 2. The isolated potassium salt, **bumetanide K**, was found to be anhydrous using thermogravimetric analysis (TGA, Fig. S1<sup>†</sup>). DVS gravimetric measurements displayed a 13% mass uptake of **bumetanide K** from 30% RH to 90% RH, signifying the formation of bumetanide potassium trihydrate, **bumetanide K(H<sub>2</sub>O)<sub>3</sub>**.<sup>18</sup> This trihydrate salt completely dehydrated upon reversing the RH to  $\leq$ 40% (Fig. 3). When form conversion was

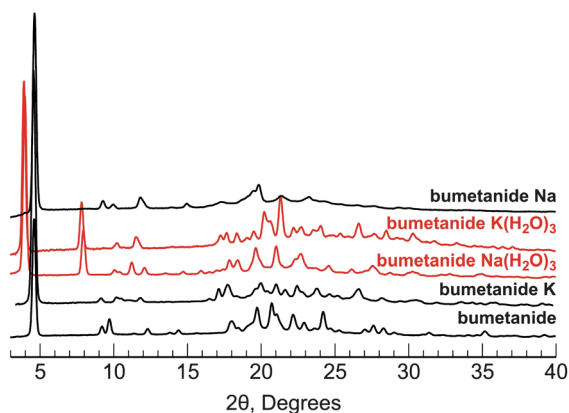


**Fig. 2** PXRD patterns of bumetanide and bumetanide salts. Patterns of the trihydrate salts are shown in red.

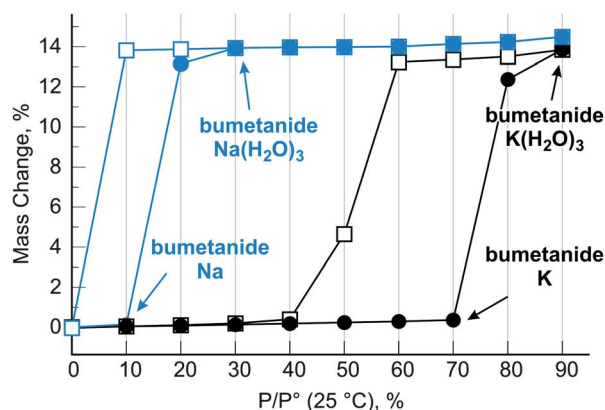


**Fig. 3** DVS gravimetry of bumetanide potassium and sodium salts at 25 °C. Filled and unfilled symbols represent sorption and desorption cycles, respectively. Each anhydrous form showed an uptake of three H<sub>2</sub>O molecules upon hydration. The theoretical weight increase for formation of trihydrates from potassium and sodium anhydrites are 13.4% and 14.0%, respectively. Changes in mass are relative to the respective anhydrous forms.

monitored at 90% RH by PXRD (Fig. S2<sup>†</sup>), new reflections of **bumetanide K(H<sub>2</sub>O)<sub>3</sub>** emerged that were consistent with the PXRD data recorded when **bumetanide K** was suspended in H<sub>2</sub>O (Fig. S3<sup>†</sup>), verifying that identical forms were produced when **bumetanide K** was exposed to conditions where water activity is high (*e.g.*, suspension in bulk water and exposure to 90% RH). A hydrated bumetanide potassium salt has been previously disclosed,<sup>19</sup> but in the absence of sufficient characterization data, no further information is available to determine the stoichiometry of waters of hydration. It is unclear whether an intermediate bumetanide potassium monohydrate was formed upon desorption of the trihydrate at 50% RH (monohydrate is theoretically 4.5% heavier than **bumetanide K**).

TGA confirmed that the isolated sodium salt was a trihydrate (**bumetanide Na(H<sub>2</sub>O)<sub>3</sub>**, Fig. S1<sup>†</sup>), which is in agreement with the reported crystal structure.<sup>13</sup> DVS measurements showed that **bumetanide Na(H<sub>2</sub>O)<sub>3</sub>** converted to anhydrous **bumetanide Na** upon evacuation from the humid atmosphere (*i.e.*,  $\leq$ 10% RH), but quantitatively recovered the 14% mass loss<sup>18</sup> upon rehydration to RH  $\geq$  20% (Fig. 3). Both bumetanide sodium and bumetanide potassium formed trihydrate salts, but each trihydrate salt differed in the humidity bracket at which the hydrates were physically stable (RH > 20% for the sodium salt and RH > 40% for the potassium salt).

TGA also showed a 12.2% decrease in mass of **bumetanide Na(H<sub>2</sub>O)<sub>3</sub>** at >80 °C (Fig. S1<sup>†</sup>), indicating the formation of anhydrous **bumetanide Na** at elevated temperatures.<sup>18</sup> The PXRD of **bumetanide Na(H<sub>2</sub>O)<sub>3</sub>** acquired at 120 °C or 0% RH (Fig. S2<sup>†</sup>) displayed similar reflections, further demonstrating that the trihydrate converts to the same anhydrous form at low humidity or elevated temperature.

### Dehydration kinetics of trihydrate salts

The activation energy ( $E_a$ ) for the dehydration of **bumetanide K(H<sub>2</sub>O)<sub>3</sub>** and **bumetanide Na(H<sub>2</sub>O)<sub>3</sub>** was extracted from the Arrhenius plots using DVS.<sup>17</sup> Dehydration was initiated by switching the humid environment surrounding the trihydrate

salts to a dry N<sub>2</sub> atmosphere. Fig. 4 shows the Arrhenius plots and Table 1 lists the isothermal *k* values between 20–30 °C and the corresponding *E<sub>a</sub>* parameter. Dehydration of both salts followed zero-order kinetics at all temperatures and the *E<sub>a</sub>* value of the potassium salt was lower than the sodium salt by 5.0 kcal mol<sup>-1</sup>.<sup>20</sup> The dehydration rate of **bumetanide K(H<sub>2</sub>O)<sub>3</sub>** was notably 15–20-fold faster than **bumetanide Na(H<sub>2</sub>O)<sub>3</sub>**, which is likely due to the 5.0-kcal mol<sup>-1</sup> difference in *E<sub>a</sub>*. The elevated *E<sub>a</sub>* barrier for dehydration of the sodium salt also suggests that the H<sub>2</sub>O molecules are bound more tightly to the crystal lattice of **bumetanide Na(H<sub>2</sub>O)<sub>3</sub>**. Such rationale is consistent with the DVS profiles in Fig. 3, which show that a lower RH is required to dehydrate **bumetanide Na(H<sub>2</sub>O)<sub>3</sub>**.

### pH-dependent solubility

The pH-solubility<sup>21</sup> profile of bumetanide in aqueous solutions at 22 °C is summarized in Table S1† and Fig. 5. As predicted, solubility is highest at pH regions where the carboxylic acid of bumetanide (p*K<sub>a</sub>* = 3.7)<sup>22</sup> is >99% ionized. Surprisingly, the solubility of the potassium salt at pH > 7.5 is five times greater compared to the sodium salt (27–30 mg mL<sup>-1</sup> vs. 5–6 mg mL<sup>-1</sup>). At the conclusion of the solubility measurements, PXRD analysis of the equilibrated solids in the suspension verified that the undissolved drug substance at pH > 7.5 was either **bumetanide Na(H<sub>2</sub>O)<sub>3</sub>** or **bumetanide K(H<sub>2</sub>O)<sub>3</sub>**, confirming that the solubility

values correspond to the trihydrate forms. Despite the increased solubility of the potassium salt, disproportionation of the salt to the free acid was not observed for suspensions stored at pH > 7.5 and 22 °C for 8 weeks. Given that the risk of salt disproportionation increases with higher solubility salts, the observations reported here bear early evidence that the potassium salt possesses the promising solution stability required to formulate a physiologically-compatible,<sup>23</sup> slightly alkaline parenteral product. At pH < 4, the sodium and potassium salts disproportionated into the free acid, causing the insoluble bumetanide to precipitate. The equilibrated forms at pH 5–7 were not determined, though it is reasonable to assume that the equilibrated suspensions consisted mixtures of the salt and free acid.

### Single-crystal structures of bumetanide K(H<sub>2</sub>O)<sub>3</sub> and bumetanide Na(H<sub>2</sub>O)<sub>3</sub>

The crystallographic data for the sodium and potassium trihydrate salts are listed in Table 2. A close examination of the PXRD patterns in Fig. 2 and the crystal data would indicate structural similarity because the unit cells show similar cell lengths and volumes, and both crystallize in monoclinic space group *C2/c*. Though the PXRD patterns additionally result in high similarity scores when compared using PXRD similarity tools, visual inspection of the patterns reveals clear differences in the two salt forms. Therefore, while it is striking that two forms

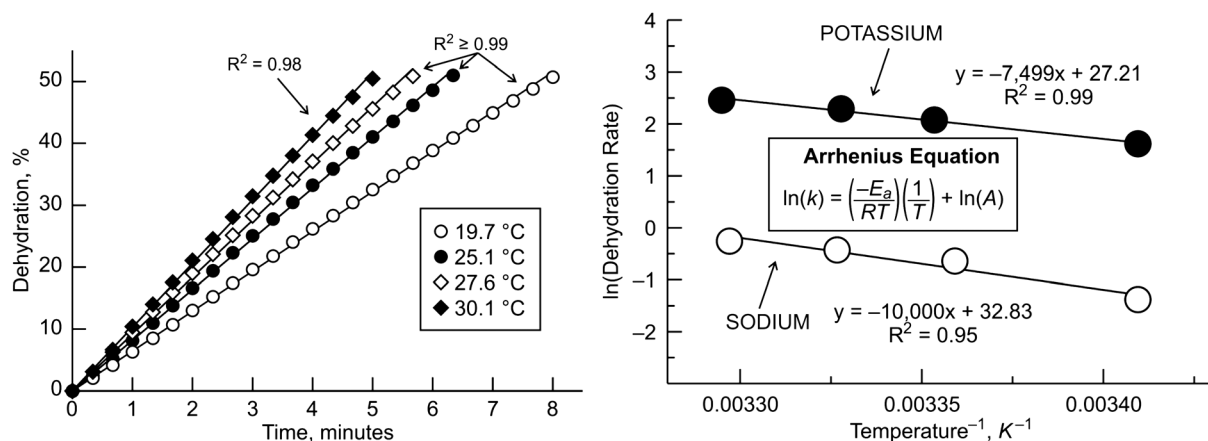


**Fig. 4** Left: Time dependence for the zero-order dehydration of **bumetanide K(H<sub>2</sub>O)<sub>3</sub>** upon exposure to dry N<sub>2</sub> in the DVS. Lines show the best fit to the zero-order kinetics. Dehydration beyond 50% is not shown due to crowding of data points. Right: Arrhenius plots for the dehydration of **bumetanide Na(H<sub>2</sub>O)<sub>3</sub>** and **bumetanide K(H<sub>2</sub>O)<sub>3</sub>**. Each point represents the average of triplicate measurements between 20 and 30 °C. Lines show best fit to the Arrhenius equation shown in the inset. The corresponding *E<sub>a</sub>* values and zero-order rates are listed in Table 1.

**Table 1** Zero-order rates (*k*) and activation energies (*E<sub>a</sub>*) for the dehydration of **bumetanide Na(H<sub>2</sub>O)<sub>3</sub>** and **bumetanide K(H<sub>2</sub>O)<sub>3</sub>**. *k* values were obtained in triplicate. *E<sub>a</sub>* was extracted from the Arrhenius plots in Fig. 4

Dehydration reaction	<i>T</i> /°C	<i>k</i> (% min <sup>-1</sup> )	<i>E<sub>a</sub></i> (kcal mol <sup>-1</sup> )
<b>bumetanide K(H<sub>2</sub>O)<sub>3</sub> → bumetanide K</b>	19.7	5.04 ± 0.05	14.9 ± 1.1
	25.1	7.99 ± 0.19	
	27.6	9.90 ± 0.24	
	30.1	11.7 ± 0.10	
<b>bumetanide Na(H<sub>2</sub>O)<sub>3</sub> → bumetanide Na</b>	19.9	0.252 ± 0.01	19.9 ± 3.3
	25.0	0.527 ± 0.02	
	27.7	0.653 ± 0.04	
	30.0	0.775 ± 0.07	

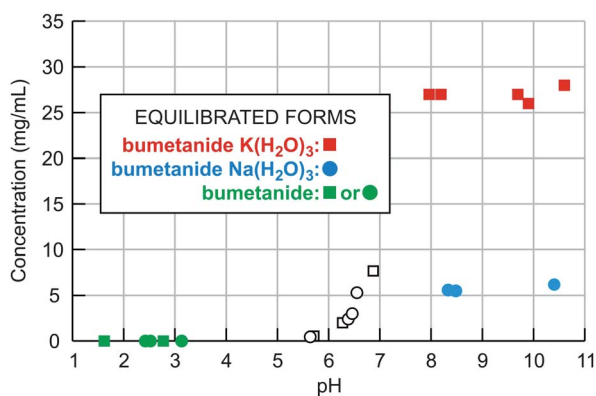


**Fig. 5** Plot of 24-h concentration vs. pH shows a marked increase in solubility of the potassium salt relative to the sodium salt at pH > 7.5. Inset shows the equilibrated forms at pH < 4 and pH > 7.5 determined by PXRD. Symbols represent the starting forms (squares: **bumetanide K**, circles: **bumetanide Na(H<sub>2</sub>O)<sub>3</sub>**) used at the start of the experiment. Raw data are listed in Table S1.†

having identical hydration states and sharing similar single-crystal structures but drastically differing in physical properties, the crystallographic data indicate that the reduced unit cells are not isostructural, and variations in crystal packing must exist. The most prominent difference in the two structures is in the arrangement of the H<sub>2</sub>O and bumetanide molecules around the potassium and sodium cations. These subtle differences in structure provide insight into the molecular basis for the dramatic differences in the material properties.

As the conformations of bumetanide in the two crystal structures overlap nearly exactly (root mean squared misfit = 0.02 Å, Fig. 6), the primary structural differences in the crystals are solely due to the placement of the cations and water molecules, likely a consequence of the larger size of the potassium cation compared with the sodium cation. The subtle differences in arrangement are evident in the packing diagrams (Fig. 7).

In **bumetanide K(H<sub>2</sub>O)<sub>3</sub>**, the K center is six-coordinated, but only one of the four H<sub>2</sub>O molecules forms a bridge with a neighboring K core. The remaining two positions are occupied by one O atom from the carbonyl group belonging to the

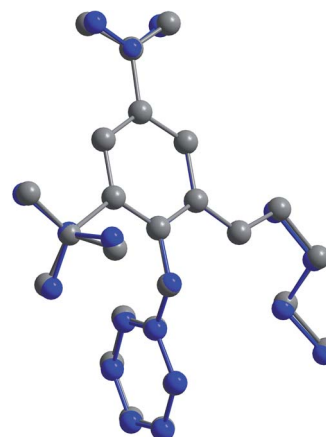


**Fig. 6** Overlay of **bumetanide Na(H<sub>2</sub>O)<sub>3</sub>** (blue) and **bumetanide K(H<sub>2</sub>O)<sub>3</sub>** (gray) shows a nearly exact superimposition of the bumetanide in the two salts.

carboxylic acid of bumetanide, and one O atom belonging to the sulfonamide moiety of bumetanide, respectively. In **bumetanide Na(H<sub>2</sub>O)<sub>3</sub>**, each six-coordinate Na center is linked to neighboring Na cores by two pairs of bridging H<sub>2</sub>O molecules. The remaining two coordination sites are occupied by a non-bridging H<sub>2</sub>O molecule and one O atom of the carboxylic moiety of bumetanide. The greater number of bridging H<sub>2</sub>O molecules in **bumetanide Na(H<sub>2</sub>O)<sub>3</sub>** provides a network of H-bonds which is considerably different to that found in **bumetanide K(H<sub>2</sub>O)<sub>3</sub>**. This network of cross-linked H<sub>2</sub>O molecules is perhaps responsible for the aforementioned discrepancy in  $\Delta E_a = 5.0 \text{ kcal mol}^{-1}$  for dehydration, and even possibly the five-fold solubility enhancement of the potassium trihydrate. Moreover, an analysis of the packing coefficients with removal of water and cation from the two crystal structures indicates that even though **bumetanide K(H<sub>2</sub>O)<sub>3</sub>** starts with a higher packing coefficient than **bumetanide Na(H<sub>2</sub>O)<sub>3</sub>**, the percentage of void space after the loss of all three H<sub>2</sub>O molecules and potassium cation differs only by 1% to that of **bumetanide Na** (Table 3). Purely from a structural perspective, **bumetanide K(H<sub>2</sub>O)<sub>3</sub>** will show more voids when it sheds water, and this looser packing during dissolution may contribute in some way to its increased solubility.

**Table 2** Crystallographic data for **bumetanide Na(H<sub>2</sub>O)<sub>3</sub>**<sup>13</sup> and **bumetanide K(H<sub>2</sub>O)<sub>3</sub>**

Compound	Bumetanide Na(H <sub>2</sub> O) <sub>3</sub>	Bumetanide K(H <sub>2</sub> O) <sub>3</sub>
Chemical formula	C <sub>17</sub> H <sub>19</sub> Na <sub>1</sub> N <sub>2</sub> O <sub>5</sub> S <sub>1</sub> ·3H <sub>2</sub> O	C <sub>17</sub> H <sub>19</sub> K <sub>1</sub> N <sub>2</sub> O <sub>5</sub> S <sub>1</sub> ·3H <sub>2</sub> O
Formula weight (g mol <sup>-1</sup> )	440.44	456.56
T/K	293	100
Wavelength (Å)	1.5418	0.71073
Crystal size/mm	0.5 × 0.4 × 0.2	0.049 × 0.077 × 0.573
Crystal system	Monoclinic	Monoclinic
Space group	C2/c	C2/c
Unit cell dimensions (Å)	<i>a</i> = 44.819(2) <i>b</i> = 5.3639(8) <i>c</i> = 17.694(4) $\beta$ = 95.91(2)°	<i>a</i> = 45.797(2) <i>b</i> = 5.4342(3) <i>c</i> = 17.5936(9) $\beta$ = 102.160(3)°
Volume/Å <sup>3</sup>	4231.2(9)	4280.3(4)
Z	8	8
Density (calculated) g cm <sup>-3</sup>	1.38	1.42
Final <i>R</i> indices	<i>I</i> > 3.0σ( <i>I</i> ) <i>R</i> <sub>1</sub> = 0.058, w <i>R</i> <sub>2</sub> = 0.059	<i>I</i> > 2.0σ( <i>I</i> ) <i>R</i> <sub>1</sub> = 0.036, w <i>R</i> <sub>2</sub> = 0.070

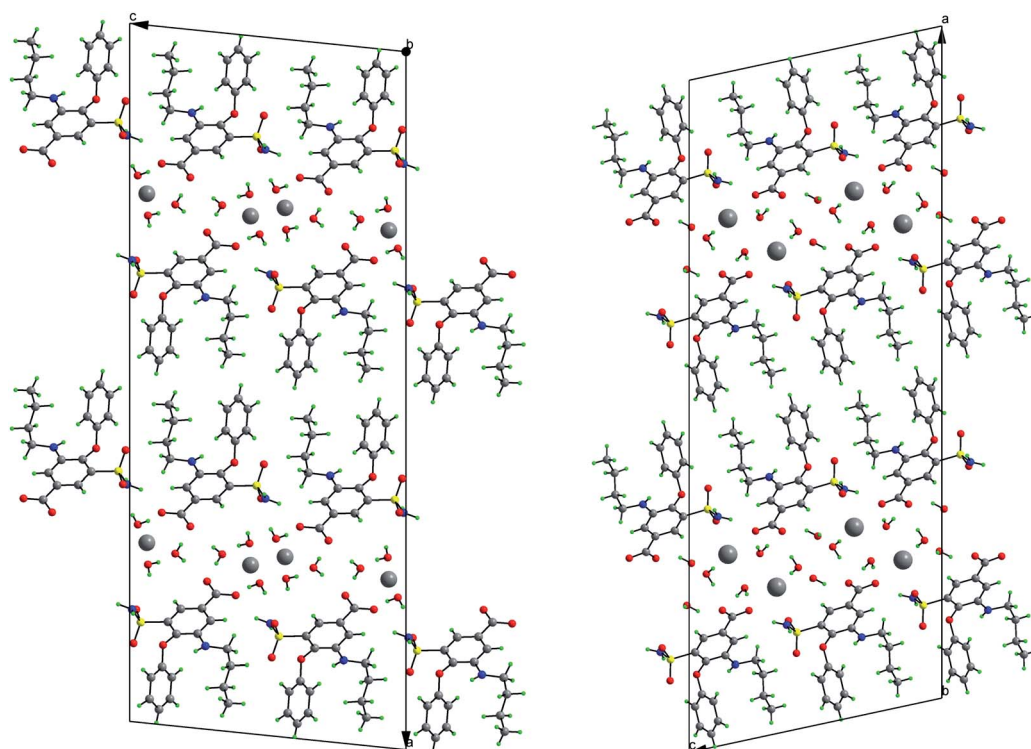


Fig. 7 Differences in crystal packing (left = bumetanide  $\text{Na}(\text{H}_2\text{O})_3$ ,<sup>13</sup> right = bumetanide  $\text{K}(\text{H}_2\text{O})_3$ ).

Table 3 Analysis of the packing coefficients with removal of water and cation from bumetanide  $\text{Na}(\text{H}_2\text{O})_3$ <sup>13</sup> and bumetanide  $\text{K}(\text{H}_2\text{O})_3$

	Bumetanide $\text{Na}(\text{H}_2\text{O})_3$ (WINJAE) <sup>13</sup> (%)	Bumetanide $\text{K}(\text{H}_2\text{O})_3$ (%)
Trihydrate + metal ion	69.3	73.6
–1 water molecule	67.5	72.6
–2 water molecules	66.1	71.0
–3 water molecules	64.0	68.7
–all water molecules and metal ion	56.3	55.6

## Conclusions

A new potassium salt trihydrate (bumetanide  $\text{K}(\text{H}_2\text{O})_3$ ) that is five times more soluble than the known bumetanide  $\text{Na}(\text{H}_2\text{O})_3$  form (27–30  $\text{mg mL}^{-1}$  vs. 5–6  $\text{mg mL}^{-1}$ ) is reported. The dehydration of the sodium salt is 15–20-fold slower than the potassium salt due to a more energetic activation barrier ( $\Delta E_a = 5.0 \text{ kcal mol}^{-1}$ ). Perhaps, the differentiated H-bond distances and crystallographic position of  $\text{H}_2\text{O}$  molecules illustrate that an obvious switch in counteranions can, and more often than not, lead to subtle changes in structure but meaningful and unpredictable variations in physicochemical properties. These data also highlight the importance of utilizing crystallography to further understand the effects of changing counterions towards the physical properties of API salts. Finally, the solubility increase for the potassium salt, which did not show evidence of disproportionation to the free acid at pH regions ( $>7$ ) where solubility exceeded  $25 \text{ mg mL}^{-1}$ , can be particularly important to low-volume parenteral formulations of bumetanide, as it facilitates the preparation of concentrated drug solutions at the near-neutral pH.

## References

- 1 M. L. Peterson, M. B. Hickey, M. J. Zaworotko and O. Almarsson, *J. Pharm. Pharm. Sci.*, 2006, **9**, 317–326.
- 2 A. T. M. Serajuddin, *Adv. Drug Delivery Rev.*, 2007, **59**, 603–616.
- 3 S. L. Childs, G. P. Stahly and A. Park, *Mol. Pharmaceutics*, 2007, **4**, 323–338.
- 4 P. H. Stahl and C. G. Wermuth, ed., *Handbook of pharmaceutical salts: properties, selection, and use*, Wiley-VCH, New York, 2002.
- 5 C. Han and B. Wang, ed., *Factors That Impact the Developability of Drug Candidates: An Overview*, in *Drug Delivery: Principles and Applications*, John Wiley & Sons, Inc., Hoboken, 2005.
- 6 C. A. Lipinski, F. Lombardo, B. W. Dominy and P. J. Feeney, *Adv. Drug Delivery Rev.*, 1997, **23**, 3–25.
- 7 L.-F. Huang and W.-Q. Tong, *Adv. Drug Delivery Rev.*, 2004, **56**, 321–334.
- 8 C. R. Gardner, C. T. Walsh and O. Almarsson, *Nat. Rev. Drug Discovery*, 2004, **3**, 926–934.
- 9 M. N. Martinez and G. L. Amidon, *J. Clin. Pharmacol.*, 2002, **42**, 620–643.
- 10 C. T. Supuran, *Curr. Pharm. Des.*, 2008, **14**, 641–648.
- 11 A. Ward and R. C. Heel, *Drugs*, 1984, **28**, 426–464.
- 12 H. W. Nielsen, E. Bechgaard, B. Twile, E. Didriksen and G. T. Almtorp, *Pharm. Dev. Technol.*, 2001, **6**, 145–149.

- 
- 13 M. Saviano, R. Fattorusso, A. Lombardi, L. Zaccaro and C. Pedone, *Acta Crystallogr., Sect. C: Cryst. Struct. Commun.*, 1995, **C51**, 395–398.
- 14 P. A. Wood, M. A. Oliveira, A. Zinkb and M. B. Hickey, *CrystEngComm*, 2012, DOI: 10.1039/C2CE06588F.
- 15 J. F. Remenar, J. M. MacPhee, B. K. Larson, V. A. Tyagi, J. H. Ho, D. A. McIlroy, M. B. Hickey, P. B. Shaw and O. Almarsson, *Org. Process Res. Dev.*, 2003, **7**, 990–996.
- 16 P. W. Betteridge, J. R. Carruthers, R. I. Cooper, K. Prout and D. J. Watkin, *J. Appl. Crystallogr.*, 2003, **36**, 1487.
- 17 J. Y. Khoo, J. Y. Y. Heng and D. R. Williams, *Ind. Eng. Chem. Res.*, 2010, **49**, 422–427.
- 18 Theoretical mass changes: bumetanide K to bumetanide  $K(H_2O)_3$  = +13.4%, bumetanide Na to bumetanide  $Na(H_2O)_3$  = +14.0%, and bumetanide  $Na(H_2O)_3$  to bumetanide Na = –12.3%.
- 19 P. W. Feit, (*Loevens Kemiske Fabrik Produktionsaktieselskab, Den.*). *Application: US*, 1976, pp. 19 pp Division of U S 13,806, p. 534
- 20 Crystal defects and particle size can influence activation energy. Both factors were not taken into consideration in this study.
- 21 The suspensions used in solubility measurements were titrated with aqueous NaOH or KOH to adjust pH. Suppression of solubility due to common-ion effect, if any, was not accounted for.
- 22 B. Song, A. K. Galande, K. Kodukula, W. H. Moos and S. M. Miller, *Drug Dev. Res.*, 2011, **72**, 315–426.
- 23 Parenteral products are generally formulated between pH 4 and 9. For examples, see R. G. Strickley, *PDA J. Pharm. Sci. Technol.*, 1999, **53**, 324–349.